Author/s:
Schenk, AK;Sear, MJ;Dontschuk, N;Tsai, A;Rietwyk, KJ;Tadich, A;Cowie, BCC;Ley, L;Stacey, A;Pakes, CI

Title:
Development of a silicon-diamond interface on (111) diamond

Date:
2020

Citation:
Schenk, A. K., Sear, M. J., Dontschuk, N., Tsai, A., Rietwyk, K. J., Tadich, A., Cowie, B. C. C., Ley, L., Stacey, A. & Pakes, C. I. (2020). Development of a silicon-diamond interface on (111) diamond. Applied Physics Letters, 116 (7), https://doi.org/10.1063/1.5144093.

RESEARCH ARTICLE | FEBRUARY 18 2020

Development of a silicon–diamond interface on (111) diamond

A. K. Schenk ; M. J. Sear ; N. Dontschuk; A. Tsai; K. J. Rietwyk; A. Tadich ; B. C. C. Cowie; L. Ley; A. Stacey; C. I. Pakes

Appl. Phys. Lett. 116, 071602 (2020)
https://doi.org/10.1063/1.5144093

Applied Physics Letters ARTICLE scitation.org/journal/apl

Development of a silicon–diamond interface on (111) diamond

Cite as: Appl. Phys. Lett. **116**, 071602 (2020); doi: 10.1063/1.5144093
Submitted: 5 January 2020 · Accepted: 4 February 2020 ·
Published Online: 18 February 2020

A. K. Schenk,[1,2,a] M. J. Sear,[1,b] N. Dontschuk,[3] A. Tsai,[3] K. J. Rietwyk,[4] A. Tadich,[1,5] B. C. C. Cowie,[5] L. Ley,[1,6] A. Stacey,[7] and C. I. Pakes[1]

AFFILIATIONS

[1]Department of Chemistry and Physics, La Trobe Institute for Molecular Science, La Trobe University, Bundoora, Victoria 3086, Australia
[2]Center for Quantum Spintronics, Department of Physics, Norwegian University of Science and Technology, NO-7491 Trondheim, Norway
[3]School of Physics, University of Melbourne, Parkville, Victoria 3010, Australia
[4]ARC Centre of Excellence in Exciton Science, Department of Chemical Engineering, Monash University, Clayton, Victoria 3800, Australia
[5]Australian Synchrotron, 800 Blackburn Road, Clayton, Victoria 3168, Australia
[6]Institut für Technische Physik, Universität Erlangen, Staudtstrasse 1, Erlangen D-91058, Germany
[7]Centre for Quantum Computation and Communication Technology, School of Physics, University of Melbourne, Parkville, Victoria 3010, Australia

[a]**Electronic mail:** A.Schenk@latrobe.edu.au
[b]**Present address:** Helmholtz-Zentrum Berlin für Materialien und Energie GmbH, Institute for Solar Fuels, Hahn-Meitner-Platz 1, D-14109 Berlin, Germany.

ABSTRACT

We report the preparation of a silicon terminated (111) diamond surface. Low energy electron diffraction and core level photoemission demonstrate that this surface is highly ordered and homogeneous and possesses a negative electron affinity. Our analysis suggests that the surface reconstruction begins with the formation of silicon trimers that coalesce into a rhombohedral 2D silicon layer reminiscent of rhombohedral silicene.

Diamond surfaces are an emerging platform for device development in many diverse applications, such as nanoscale electro/magnetometry,[1,2] biosensing,[3–6] cold cathode electron emitters,[7–9] and spintronics.[10–13] The suitability of diamond surfaces for such a broad variety of applications is a result of the ability to significantly alter the electronic and interfacial properties of the diamond surface by simply changing the terminating chemical species, allowing the surface properties to be engineered and optimized for a specific application.

In recent years, silicon[14] and germanium[15] terminated (100) diamond surfaces have been developed. These terminations offer atomically flat terraces, which have previously been associated only with the hydrogen-terminated (100) diamond surface. Additionally, they possess dangling bonds that allow further chemical modification of the surface without the harsh chemical and plasma treatments that are typical for diamond. The silicon terminated (100) diamond surface forms an ordered oxide[16] and fluoride,[17] has a higher thermal stability than other (100) diamond surface terminations,[18] and possesses a negative electron affinity.[19] Furthermore, the oxidized Si termination can be doped to produce p-type surface conductivity.[20] These findings show that group IV terminated diamond surfaces continue the trend of diamond surfaces in offering diverse properties of interest for device applications, motivating further exploration.

The relative ease of producing high quality (100) diamond films has made it the frequent subject of surface investigations; however, (111) diamond offers possibilities that (100) diamond does not. The (111) diamond surface—herein also referred to as the C(111) surface—has hexagonal symmetry with three rotationally equivalent domains, allowing the formation of surface bonding geometries that may not exist on the group IV terminated (100) diamond surface. Notably, recent theoretical work suggests that the C(111) surface may

allow the formation of silicene phases.[21] Additionally, (111) oriented crystals allow for the preferential alignment of near-surface defects during growth[22] and the optimal alignment of defect dipoles with surface targets and structures.[23] For architectures relying on near-surface nitrogen vacancy centers, it is desirable to produce terminated surfaces with new chemical functionality,[24] electronic properties,[25] and a high degree of order and homogeneity[26] while avoiding surface defects.[27] Here, we demonstrate that the C(111) surface can be functionalized with silicon using a self-assembly method. Our measurements indicate that this process yields a highly ordered and chemically homogeneous surface with a rhombohedral arrangement of silicon bound to the diamond surface, in apparent agreement with the rhombohedral silicene structure proposed by Xu *et al.*[21]

We have used boron-doped, CVD type IIb (111) diamond, with a boron density sufficient to prevent charging during measurements. The sample was hydrogen terminated *ex situ* in a microwave hydrogen plasma for 5 min at 80 Torr, with the sample maintained at a temperature of approximately 850 °C, and then transferred to the endstation at the Soft x-ray Spectroscopy (SXR) beamline of the Australia Synchrotron and inserted into the ultra-high vacuum endstation, where the remaining preparation and characterization were carried out *in situ*. The endstation has a SPECS Phoibos 150 hemispherical analyzer for performing high resolution core-level photoelectron spectroscopy (XPS), a reverse-optics Low Energy Electron Diffraction (LEED) system for monitoring surface reconstruction, and a Kelvin Probe (KP Technology) allowing the characterization of the contact potential difference (CPD). The sample was mounted inside a Ta envelope on a sample holder with an underlying electron beam heater. A K-type thermocouple in direct contact with the envelope and an optical pyrometer were used simultaneously to monitor the sample temperature during annealing. All measurements were performed at pressures below 5×10^{-10} mbar. High resolution XPS measurements of the C1s and Si2p core levels were performed using photon energies of 350 eV and 150 eV, respectively, to maximize the surface sensitivity. The binding energy (BE) scale of all spectra is referenced to the Fermi level of a gold foil in electrical contact with the sample by setting the $Au4f_{7/2}$ core-level BE to 84.00 eV. Core level spectra were fitted with symmetric Voigt components with Lorentzian widths of 0.15 eV for C1s[28] and 0.055 eV for Si2p[29] after applying a Shirley background correction.[30] Fits of Si2p were restrained to ensure a spin–orbit splitting of 0.60 eV and a branching ratio of 2:1.[29]

Once in vacuum, the sample was annealed at 450 °C, for 1 h, producing a clean (1×1) hydrogen terminated surface, as confirmed by XPS and LEED.[28] The hydrogen was desorbed from the surface by annealing at 950 °C for 30 min.[28] Silicon was deposited onto the bare (111) surface by passing current through a silicon wafer until it sublimed, followed by annealing the sample to 900–950 °C, for 10 min. As in previous work,[14] photoelectron attenuation was used to estimate the quantity of silicon deposited from the ratio of C1s and Si2p measured with a photon energy of 400 eV, which agreed well with the coverage determined from the reduction of the π peak (associated with the bare diamond surface) in the valence band; these coverages are tabulated in Table I. Coverages are given as a fraction of the C(111) surface density—i.e., a coverage of 1 ML is equivalent to 1 silicon atom per surface carbon atom.

Figures 1(a) and 1(b) show the valence band and the pre-edge region of the carbon K-edge near edge x-ray adsorption fine structure (NEXAFS) spectra, respectively; the full NEXAFS spectra are included in the supplementary material. Spectroscopy on the bare (111) diamond surface shows strong resonances associated with the π bonded Pandey chain reconstruction,[31,32] which are seen to decrease as silicon is added to the surface. This suggests that the silicon breaks the π bonding of the Pandey chain reconstruction. This interpretation is confirmed by the C1s XPS spectra acquired throughout the experiment, shown in Fig. 1(c). The core level of the bare (111) surface (0 ML) contains two components $B_{(2\times1)}$ and $C_{(2\times1)}$ (chemical shift -0.72 ± 0.05 eV relative to $B_{(2\times1)}$), with the former attributed to the diamond bulk and the latter attributed to the (2×1) reconstructed surface carbon atoms.[28] These two components decrease in intensity with silicon uptake and annealing, and three additional components (C_{Si1}, C_{Si2}, and B_{Si}) develop within the core level. When we consider the inductive effect,[33] the strong chemical shift of C_{Si1} (-0.97 ± 0.05 eV) and C_{Si2} (-1.42 ± 0.05 eV) relative to the diamond bulk $B_{(2\times1)}$ indicates that these carbon atoms are becoming more electron-rich than $C_{(2\times1)}$, from which we infer that they are surface carbon atoms participating in carbon–silicon bonds. We attribute the C_{Si1} component to carbon atoms participating in a single C–Si bond, while the larger shift of C_{Si2} indicates that this component represents carbon atoms bonded to multiple silicon atoms or forming double bonds with a single silicon atom. As will become apparent, we believe that the C_{Si1} species is part of a regular reconstruction, while the less populated C_{Si2} species is carbon atoms at step edges or surface defect sites bonding with silicon in alternative configurations. The final component B_{Si} (chemical shift -0.42 ± 0.05 eV relative to $B_{(2\times1)}$) is attributed to bulk carbon atoms lying beneath those areas of the surface to which silicon has bonded, as the intensity of this component increases, while the intensity of the $B_{(2\times1)}$ component decreases.

TABLE I. Silicon coverages calculated using Eq. (2) and the C1s XPS spectra, compared to those calculated using photoelectron attenuation (attenuation), and calculated from the intensity reduction of the π peak in the valence band (VB).

Attenuation	VB	Equation (2) ($\alpha = 1$, $\beta = 3$)
0.62 ± 0.06 ML	0.64 ± 0.06 ML	0.64 ± 0.06 ML
0.78 ± 0.08 ML	0.72 ± 0.07 ML	0.71 ± 0.07 ML
1.00 ± 0.10 ML	1.00 ± 0.10 ML	0.97 ± 0.10 ML

The surface electron affinity χ at each stage of the experiment is shown in Fig. 1(c). This has been calculated with the method applied in previous investigations,[19,34] which uses the sample work function Φ_D, determined from calibrated CPD measurements with the Kelvin probe, the separation between the diamond Fermi level and valence band maximum ($E_F - E_{VBM}$), and the diamond bandgap E_G, combined using the following equation:

$$\chi = \Phi_D + (E_F - E_{VBM}) - E_G. \quad (1)$$

The separation ($E_F - E_{VBM}$) is typically calculated from the position of the bulk C1s component, using the constant separation between the bulk C1s and the valence band maximum for diamond found by Maier *et al.*[35] In our case, where the bulk core level is bifurcated, we have used the bulk component areas to determine a weighted average bulk position and, from this, calculated ($E_F - E_{VBM}$); this is a reasonable approach given that the measured CPD is determined by a spatial

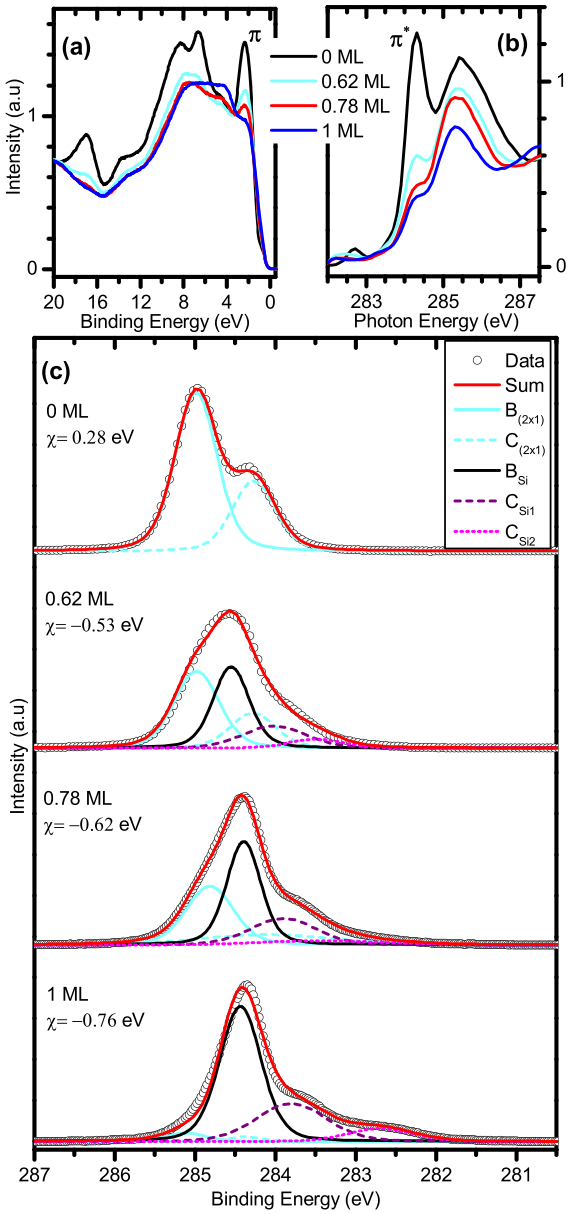

FIG. 1. Evolution of the valence band ($\hbar\omega = 100$ eV) (a), grazing-incidence carbon K-edge NEXAFS (b), and C1s core level XPS (c) with silicon uptake on the (111) diamond surface. Indicated silicon coverages are based on photoelectron attenuation calculations. χ is the electron affinity measured using the method described in the text.

average. This analysis shows that the electron affinity begins at +0.28 eV for the bare (111) diamond surface and transitions to a negative electron affinity of −0.76 eV for a full monolayer silicon coverage, with an experimental uncertainty of ±0.10 eV for all electron affinities.

An example of the Si2p core levels acquired during this experiment is presented in Fig. 2. At all coverages, the Si2p core level contains two chemical components (Si1 and Si2) separated by

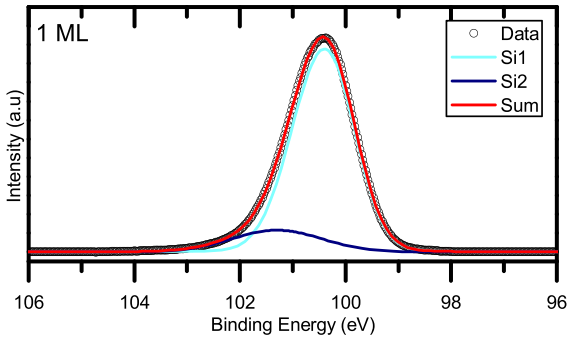

FIG. 2. The Si2p core level recorded at 1 ML silicon coverage in this experiment; for clarity, the individual spin–orbit components ($Si2p_{3/2}$ and $Si2p_{1/2}$) are not shown.

0.87 ± 0.05 eV, and we attribute both components to silicon atoms participating in carbon–silicon bonding. When interpreted within the context of the inductive effect,[33] the higher binding energy of the Si2 component indicates that the silicon atoms in this environment are more electron deficient than the those in the Si1 environment. As carbon–silicon bonds will withdraw electron density from silicon atoms, this indicates that the atoms in the Si2 chemical environment form more carbon–silicon bonds than those in the Si1 environment. Accordingly, we attribute the Si1 component to silicon atoms participating in a single C–Si bond, while the Si2 component is attributed to silicon atoms bonding with more than one carbon atom or participating in double-bonding, and note that the relative intensity of the Si2 component increases with silicon coverage from 6% at 0.62 ML to 14% at 1 ML.

Having demonstrated that silicon bonds to the C(111) surface, we now turn to exploring the arrangement of silicon. Figure 3 shows the LEED patterns recorded at each stage of silicon deposition. Panel (a) shows the expected (2×1) pattern for the Pandey chain reconstruction of the bare (111) diamond surface;[36] the weak $(\frac{1}{2}\frac{1}{2})$ spots (highlighted with a square) are typical of bare (111) surfaces[37] and result from domains of different Pandey chain orientations. At low silicon coverage, the LEED pattern remains identical to the bare surface, apart from a slight increase in the background signal (see the supplementary material for LEED at 0.22 ML coverage). However, the pattern recorded at 0.62 ML [Fig. 3(b)] shows new spots appearing in the $(\frac{1}{3}\frac{1}{3})$ positions (highlighted by triangles), which are characteristic of a $(\sqrt{3} \times \sqrt{3})R30°$ reconstruction, while the (2×1) spots remain. The C(111) surface has a pair of known $(\sqrt{3} \times \sqrt{3})R30°$ reconstructions characterized by adlayer trimers—previously, these have been carbon trimers.[38,39] As carbon and silicon share a valence, we propose that the same trimer bonding configuration is possible for silicon on C(111). The arrangement of spots at 0.78 ML [Fig. 3(c)] remains the same, although the intensity of the $(\frac{1}{2}\frac{1}{2})$ spots has increased relative to the rest of the pattern, and by 1 ML [Fig. 3(d)], the LEED pattern is (2×2), with the $(\frac{1}{3}\frac{1}{3})$ spots having disappeared completely. The LEED pattern evolution with coverage suggests the initial formation of a short-range ordered structure, which gives a $(\sqrt{3} \times \sqrt{3})R30°$ pattern, before coalescing into a structure, which produces the (2×2) pattern. A pathway to such an evolution is indicated in Fig. 3(f), where isolated silicon trimers are initially formed. With increasing coverage,

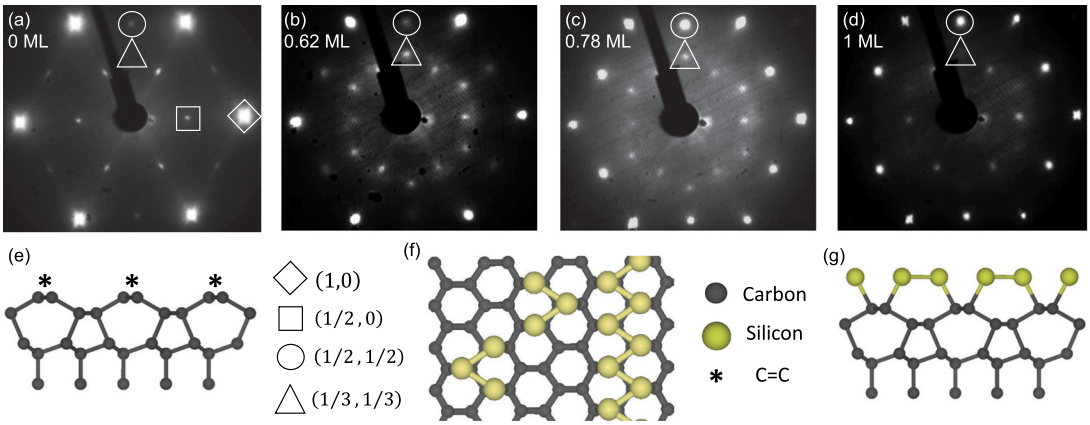

FIG. 3. LEED patterns acquired at 70 eV at each stage of this experiment: (a) bare (111) diamond, (b)–(d) increasing silicon uptake, (e) the Pandey chain reconstruction of the bare (111) surface, and (f) and (g) the proposed model for the reconstruction. The spot positioning and reconstruction are discussed in the text.

these trimers will begin forming patches of a rhombohedral silicon arrangement, yielding a (2×2) LEED pattern for the overall surface reconstruction; Fig. 3(g) shows the side-on view of the atomic arrangement. Such a structure is reminiscent of rhombohedral silicene, which recent theoretical work suggests may form on (111) oriented diamond.[21]

However, the proposed reconstruction model has only a single chemical environment for surface carbon and silicon atoms, in which they are participating in a single heteroatomic bond, while our XPS indicates two chemical environments for both carbon and silicon. As we have established, the minority surface species (C_{Si2} and Si2) in both core levels can reasonably be attributed to atoms participating in more than one carbon–silicon bond, while the majority species (C_{Si1} and Si1) fit the requirements of the (2×2) rhombohedral unit cell arrangement presented in Figs. 3(f) and 3(g). Three explanations for C_{Si2} and Si2 present themselves are as follows: (i) an additional chemical species exists within the (2×2) unit cell, (ii) a coexisting reconstruction containing C_{Si2} and Si2, or (iii) species randomly distributed on the surface, which will not contribute to LEED. As C_{Si2} and Si2 do not grow in direct proportion to C_{Si1} and Si1, we can infer that the multiple-bonded species are not a regular aspect of the (2×2) rhombohedral unit cell. Given that we observe a clear, sharp (2×2) LEED pattern with no additional spots, it is difficult to justify the existence of a coexisting reconstruction, although this cannot be definitively ruled out. The third possibility is the most credible. Diamond surfaces typically contain high surface defect and step edge densities,[40,41] allowing bonding arrangements to form, which do not exist on the atomically flat terraces, and these secondary chemical environments would be randomly distributed and thus not contribute to the LEED pattern. On this basis, we propose that the surface reconstruction is a (2×2) rhombohedral unit cell, assigning the chemical environments C_{Si1} and Si1 to atoms in this reconstruction, while the C_{Si2} and Si2 components are the result of silicon atoms facilitating step-edge reconstruction and satisfying defect sites in the surface.

If we continue with the rhombohedral reconstruction model, an alternative means of calculating the surface coverage θ can be devised from the intensity of the C1s components $C_{(2\times1)}$, C_{Si1}, and C_{Si2}

$$\theta = 1 - \frac{C_{(2\times1)}}{C_{(2\times1)} + \alpha C_{Si1} + \beta C_{Si2}}, \tag{2}$$

where the component labels indicate the component intensities, and α and β are the number of silicon atoms associated with each carbon atom, on average, for the chemical environments C_{Si1} and C_{Si2}. For the rhombohedral model, α is 1, and setting β to 3 gives the coverages presented in Table I, which agree well with the coverages calculated by photoelectron attenuation and from the intensity reduction of the π peak in the valence band. While this does not confirm our proposed model, it does lend credibility to our arguments that our observations can be explained within a simple, consistent model.

In summary, we report a self-assembly method for functionalizing the (111) diamond surface with silicon. Core level photoemission confirms that silicon has bonded to the bare (111) diamond surface after annealing to 950 °C. The resulting surface is highly ordered, with a (2×2) LEED pattern at a full monolayer surface coverage, and silicon termination produces a transition from the positive +0.28 eV electron affinity of the bare (111) surface to a negative electron affinity of −0.76 eV at a silicon coverage of 1 ML. Our results can be consistently explained by a reconstruction where silicon atoms initially form trimers on the surface, coalescing into a rhombohedral layer of silicon. Such an arrangement of silicon on (111) diamond was predicted by recent theoretical work[21] and attributed to a rhombic silicene-like phase possessing a 2D metallic character. While further characterization, such as scanning tunneling microscopy/spectroscopy and electrical transport measurements, is needed to determine the exact atomic structure of the reconstruction and confirm the nature of the electronic structure, the experimental realization of such a 2D bound phase of silicon on diamond may open possibilities for spintronics.

See the supplementary material for the 275–330 eV NEXAFS spectra and LEED at 0.22 ML silicon coverage.

This research was undertaken using the Soft x-ray Spectroscopy beamline at the Australian Synchrotron, part of ANSTO. This work was performed in part at the Melbourne Centre for Nanofabrication (MCN) in the Victorian Node of the Australian

National Fabrication Facility (ANFF). This work was supported by the Australian Research Council through Grant Nos. DP150101673, CE170100012, and CE170100026. This work was supported by the Research Council of Norway through its Centres of Excellence funding scheme, Project No. 262633, "QuSpin," and the Fripro program, Project No. 250985 "FunTopoMat."

REFERENCES

[1]R. Schirhagl, K. Chang, M. Loretz, and C. L. Degen, Annu. Rev. Phys. Chem. **65**, 83 (2014).
[2]M. Loretz, S. Pezzagna, J. Meijer, and C. Degen, Appl. Phys. Lett. **104**, 033102 (2014).
[3]G. Balasubramanian, A. Lazariev, S. R. Arumugam, and D.-W. Duan, Curr. Opin. Chem. Biol. **20**, 69 (2014).
[4]Y. Wu, F. Jelezko, M. B. Plenio, and T. Weil, Angew. Chem., Int. Ed. **55**, 6586 (2016).
[5]W. Yang and R. J. Hamers, Appl. Phys. Lett. **85**, 3626 (2004).
[6]I. Lovchinsky, A. Sushkov, E. Urbach, N. P. de Leon, S. Choi, K. De Greve, R. Evans, R. Gertner, E. Bersin, C. Müller *et al.*, Science **351**, 836 (2016).
[7]N. Xu and S. E. Huq, Mater. Sci. Eng. R: Rep **48**, 47 (2005).
[8]K. Okano, S. Koizumi, S. R. P. Silva, and G. A. Amaratunga, Nature **381**, 140 (1996).
[9]M. Geis, N. Efremow, J. Woodhouse, M. McAleese, M. Marchywka, D. Socker, and J. Hochedez, IEEE Electron Device Lett. **12**, 456 (1991).
[10]G. Akhgar, D. L. Creedon, L. H. Willems van Beveren, A. Stacey, D. I. Hoxley, J. C. McCallum, L. Ley, A. R. Hamilton, and C. I. Pakes, Appl. Phys. Lett. **112**, 042102 (2018).
[11]G. Akhgar, O. Klochan, L. H. Willems van Beveren, M. T. Edmonds, F. Maier, B. J. Spencer, J. C. McCallum, L. Ley, A. R. Hamilton, and C. I. Pakes, Nano Lett. **16**, 3768 (2016).
[12]M. T. Edmonds, L. H. Willems van Beveren, O. Klochan, J. Cervenka, K. Ganesan, S. Prawer, L. Ley, A. R. Hamilton, and C. I. Pakes, Nano Lett. **15**, 16 (2015).
[13]J. Cai, A. Retzker, F. Jelezko, and M. B. Plenio, Nat. Phys. **9**, 168 (2013).
[14]A. Schenk, A. Tadich, M. Sear, K. M. O'Donnell, L. Ley, A. Stacey, and C. Pakes, Appl. Phys. Lett. **106**, 191603 (2015).
[15]M. J. Sear, A. K. Schenk, A. Tadich, B. J. Spencer, C. A. Wright, A. Stacey, and C. I. Pakes, J. Phys.: Condens. Matter **29**, 145002 (2017).
[16]A. Schenk, M. Sear, A. Tadich, A. Stacey, and C. Pakes, J. Phys.: Condens. Matter **29**, 025003 (2017).
[17]A. K. Schenk, M. J. Sear, N. Dontschuk, A. Tadich, A. Stacey, and C. I. Pakes, "Fluorination of the silicon-terminated (100) diamond surface via decomposition of $C_{60}F_{48}$" (unpublished).
[18]M. J. Sear, A. K. Schenk, A. Tadich, A. Stacey, and C. I. Pakes, Phys. Status Solidi A **215**, 1800283 (2018).
[19]A. Schenk, A. Tadich, M. Sear, D. Qi, A. Wee, A. Stacey, and C. Pakes, Nanotechnology **27**, 275201 (2016).
[20]M. J. Sear, A. K. Schenk, A. Tadich, A. Stacey, and C. I. Pakes, Appl. Phys. Lett. **110**, 011605 (2017).
[21]R. Xu, N. Gao, H. Li, D. Qiu, Q. Wang, and S. Cheng, Phys. Chem. Chem. Phys. **20**, 21699 (2018).
[22]J. Michl, T. Teraji, S. Zaiser, I. Jakobi, G. Waldherr, F. Dolde, P. Neumann, M. W. Doherty, N. B. Manson, J. Isoya *et al.*, Appl. Phys. Lett. **104**, 102407 (2014).
[23]E. Neu, P. Appel, M. Ganzhorn, J. Miguel-Sánchez, M. Lesik, V. Mille, V. Jacques, A. Tallaire, J. Achard, and P. Maletinsky, Appl. Phys. Lett. **104**, 153108 (2014).
[24]A. Krueger and D. Lang, Adv. Funct. Mater. **22**, 890 (2012).
[25]M. Kaviani, P. Deak, B. Aradi, T. Frauenheim, J.-P. Chou, and A. Gali, Nano Lett. **14**, 4772 (2014).
[26]S. Sangtawesin, B. L. Dwyer, S. Srinivasan, J. J. Allred, L. V. Rodgers, K. De Greve, A. Stacey, N. Dontschuk, K. M. O'Donnell, D. Hu *et al.*, arXiv:1811.00144 (2018).
[27]A. Stacey, N. Dontschuk, J.-P. Chou, D. A. Broadway, A. K. Schenk, M. J. Sear, J.-P. Tetienne, A. Hoffman, S. Prawer, C. I. Pakes *et al.*, Adv. Mater. Interfaces **6**, 1801449 (2019).
[28]R. Graupner, F. Maier, J. Ristein, L. Ley, and C. Jung, Phys. Rev. B **57**, 12397 (1998).
[29]R. Hunger, R. Fritsche, B. Jaeckel, W. Jaegermann, L. J. Webb, and N. S. Lewis, Phys. Rev. B **72**, 045317 (2005).
[30]D. A. Shirley, Phys. Rev. B **5**, 4709 (1972).
[31]R. Graupner, M. Hollering, A. Ziegler, J. Ristein, L. Ley, and A. Stampfl, Phys. Rev. B **55**, 10841 (1997).
[32]R. Graupner, J. Ristein, L. Ley, and C. Jung, Phys. Rev. B **60**, 17023 (1999).
[33]K. Gao, T. Seyller, and L. Ley, Solid State Commun. **139**, 370 (2006).
[34]K. M. O'Donnell, M. T. Edmonds, A. Tadich, L. Thomsen, A. Stacey, A. Schenk, C. I. Pakes, and L. Ley, Phys. Rev. B **92**, 035303 (2015).
[35]F. Maier, J. Ristein, and L. Ley, Phys. Rev. B **64**, 165411 (2001).
[36]T. Frauenheim, U. Stephan, P. Blaudeck, D. Porezag, H.-G. Busmann, W. Zimmermann-Edling, and S. Lauer, Phys. Rev. B **48**, 18189 (1993).
[37]J. Lander and J. Morrison, Surf. Sci. **4**, 241 (1966).
[38]M. Sternberg, T. Frauenheim, W. Zimmermann-Edling, and H.-G. Busmann, Surf. Sci. **370**, 232 (1997).
[39]G. Kern, J. Hafner, and G. Kresse, Surf. Sci. **366**, 464 (1996).
[40]A. K. Schenk, K. J. Rietwyk, A. Tadich, A. Stacey, L. Ley, and C. I. Pakes, J. Phys.: Condens. Matter **28**, 305001 (2016).
[41]L. Ley, Diamond Relat. Mater. **20**, 418 (2011).